

Special Article

Imaging of Atherosclerosis: Invasive and Noninvasive Techniques

JOËLLA E. VAN VELZEN^{1,2}, JOANNE D. SCHUIJF¹, FLEUR R. DE GRAAF¹, J. WOUTER JUKEMA^{1,2}, ALBERT DE ROOS³, LUCIA J. KROFT³, MARTIN J. SCHALIJ¹, JOHANNES H.C. REIBER³, ERNST E. VAN DER WALL^{1,2}, JEROEN J. BAX¹

¹Department of Cardiology, Leiden University Medical Center, Leiden, ²Interuniversity Cardiology Institute, Utrecht, ³Department of Radiology, Leiden University Medical Center, Leiden, The Netherlands

Key words:
Coronary artery disease, atherosclerosis, imaging.

Address:

Jeroen J. Bax

Leiden University
Medical Center,
Department of
Cardiology,
Albinusdreef 2,
P.O. Box 9600, 2300 RC
Leiden,
The Netherlands
e-mail:
j.j.bax@lumc.nl

Coronary artery disease (CAD), or narrowing of the coronary arteries due to atherosclerosis, remains one of the leading causes of morbidity and mortality worldwide. However, a substantial number of patients who present with an acute coronary event due to rupture or erosion of an atherosclerotic plaque do not experience any prior symptoms. This observation emphasizes the need to improve the early detection of atherosclerosis. Traditionally, imaging of the coronary arteries has focused on the assessment of luminal dimensions and the presence of severe stenosis by means of invasive coronary angiography. However, invasive coronary angiography can only assess the degree of stenosis and is less suited to evaluate the presence of atherosclerosis, including the presence of (potentially high-risk) plaques. As a result, there is an emerging need for imaging modalities that can identify atherosclerotic plaques with high-risk features indicating increased vulnerability. In this regard particularly, noninvasive techniques may be valuable, as they may identify high-risk patients at a relatively early stage and may provide the opportunity for novel treatment strategies. Additionally, noninvasive imaging techniques may be used to monitor progression and/or regression of coronary atherosclerosis and thus possibly to evaluate the effectiveness of anti-atherosclerotic therapies on a larger scale.

Accordingly, the present review will

focus on invasive and noninvasive imaging modalities for the evaluation of atherosclerosis and detection of vulnerable lesions in the coronary arteries.

Characteristics of the potentially “vulnerable plaque”

Due to the lack of prospective data and natural history studies, most details concerning the potentially vulnerable plaque have been derived from retrospective post-mortem studies.¹⁻³ It has been established that the majority of acute coronary events (>70%) are caused by plaque rupture followed by thrombus formation.³ The most common substrate for superimposed thrombus formation is presumed to be the thin-capped fibroatheroma; a plaque with a large necrotic core and thin fibrous cap (<65 µm thick) infiltrated by macrophages and lymphocytes (Figure 1).⁴ The thin fibrous cap contains a decreased smooth muscle content, which in certain circumstances can rupture and cause the thrombogenic parts of the plaque to be exposed into the lumen. This subsequently leads to the activation of the clotting cascade and the formation of a thrombus that can compromise the lumen, resulting in an acute coronary syndrome (ACS). In the remaining ~30% of acute coronary events, thrombosis may be due to other causes than plaque rupture, including plaque erosion, intraplaque hemorrhage and calcified

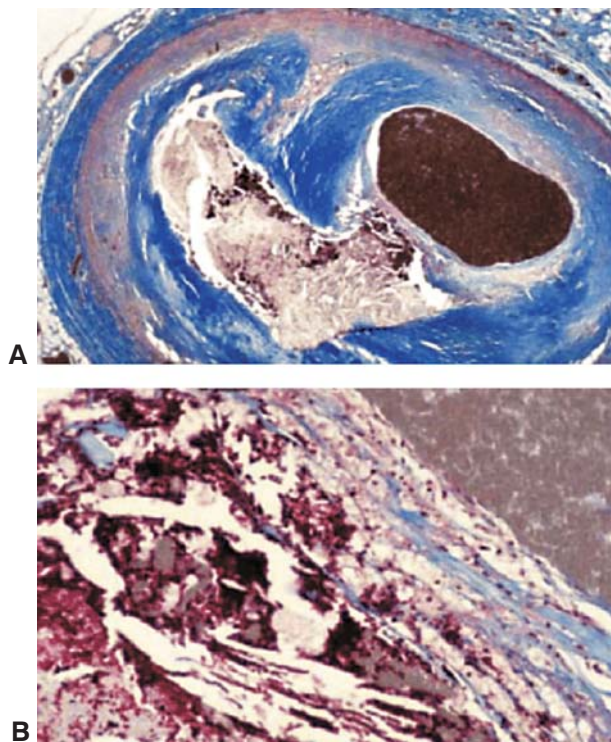


Figure 1. Histological specimen of inflamed thin-capped fibroatheroma with trichrome stain, rendering lipid colorless, collagen blue and erythrocytes red. A: Atherosclerotic coronary artery containing a large lipid core and thin fibrous cap, with postmortem injected contrast in lumen. B: Detail of the fibrous cap, demonstrating that the cap is heavily inflamed. The fibrous cap consists of many macrophages and within the necrotic core extravasated erythrocytes can be seen, indicating a possible plaque rupture. Reprinted with permission from Schaar et al.⁴

nodules.³ The various atherosclerotic lesions and their association with thrombus are described in Table 1.

Additional characteristics of plaques prone to rupture include large plaque volume, positive remodeling, presence of microcalcifications and proximal location of the lesion. It has still not been fully elucidated which trigger actually causes the plaque to rupture, although it has been postulated that inflammation plays a critical role. Indeed, as shown by studies assessing macrophage infiltration in particular, the fibrous cap is locally deeply inflamed (Figure 1).⁵ Inflammation is often a result of endothelial dysfunction. Initially, endothelial dysfunction results from a disturbance in blood flow (flow reversal or oscillating shear stress) at bifurcations or tortuousness of vessels.⁶ However, it has been suggested that not only blood flow disturbances, but also cardiovascular risk factors such as hypercholesterolemia, smoking and diabetes, can induce endothelial dysfunction.^{7,8} Due to

endothelial cell activation, the increased expression of adhesion molecules (e.g. selectins, vascular cell adhesion molecules [VCAMs], and intercellular adhesion molecules [ICAMs]) promotes the infiltration and homing of monocytes. Consequently, the monocytes migrate into the plaque and convert into macrophages, contributing to the process of atherogenesis.⁷

At present, there is no widely accepted diagnostic technique for the identification of vulnerable plaques. However, several invasive and noninvasive imaging modalities are currently under development that may to some extent allow the detection of plaques prone to rupture.

Invasive imaging of atherosclerotic plaques

Invasive coronary angiography

Invasive coronary angiography is currently the gold standard for the diagnosis of CAD and provides an accurate and detailed overview of the anatomy of the coronary artery tree, including precise quantification of the degree of stenosis. Accordingly, the technique is extensively used to guide further treatment strategies, such as coronary angioplasty or bypass surgery.

However, the evaluation of percentage diameter stenosis has limited value in predicting future cardiac events. Indeed, as demonstrated during the follow up of patients admitted for acute myocardial infarction, almost two thirds of plaques prone to rupture were located in non flow-limiting atherosclerotic lesions, and only a minority were located in severely obstructed lesions.^{9,10} Although the likelihood of occlusion for an individual lesion is directly related to the severity of stenosis, non-obstructive lesions are far more common and thus may frequently cause coronary occlusion due to their greater number (Figure 2). Accordingly, evaluation of the percentage diameter stenosis by means of invasive coronary angiography does not allow differentiation between stable and unstable plaques.

Notably, novel promising angiographic acquisition approaches have been developed recently. One of these acquisition methods is rotational 3-dimensional coronary angiography, a new imaging technique in which the gantry is mechanically rotated around the patient, providing a multitude of X-ray projections during a single contrast injection.¹¹ Using this technique, motion information about the coronary arteries can be extracted, including vessel dis-

Table 1. Morphological description of atherosclerotic lesions. Table modified from Virmani et al.³

Lesion name	Lesion description	Thrombus
Non-atherosclerotic intimal lesions: Intimal thickening	Normal accumulation of SMCs in the intima without lipid or macrophage foam cells	Absent
Intimal xanthoma	Subendothelial accumulation of foam cells in intima without necrotic core or fibrous cap	Absent
Progressive atherosclerotic lesions: Pathologic intimal thickening With erosion	SMCs in proteoglycan-rich matrix with areas of extracellular lipid accumulation without necrosis Luminal thrombosis; plaque same as above	Absent Thrombus most often mural and infrequently occlusive
Fibrous cap atheroma With erosion	Well-formed necrotic core with overlying fibrous cap Luminal thrombosis; plaque same as above, no communication of thrombus with necrotic core	Absent Thrombus most often mural and infrequently occlusive
TCFA With rupture	Thin fibrous cap infiltrated with macrophages and lymphocytes, rare SMCs, and an underlying necrotic core Fibroatheroma with cap disruption; luminal thrombus communicates with underlying necrotic core	Absent, with intraplaque hemorrhage/fibrin Thrombus usually occlusive
Calcified nodule Fibrocalcific plaque	Eruptive nodular calcification with underlying fibrocalcific plaque Collagen-rich, usually with significant stenosis; large areas of calcification with few inflammatory cells, necrotic core	Thrombus usually non-occlusive Absent

SMC – smooth muscle cell; TCFA – thin-capped fibroatheroma.

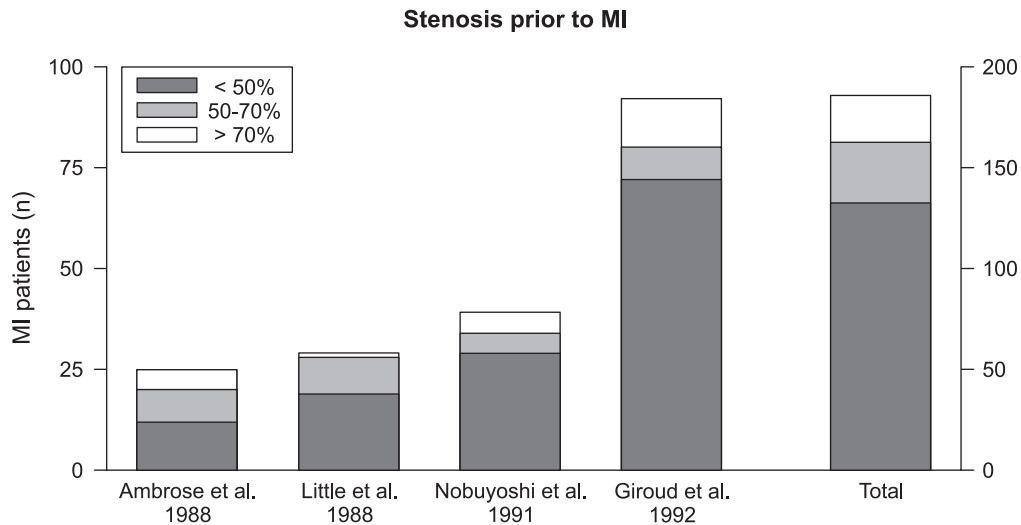


Figure 2. Bar charts representing stenosis severity and related risk of myocardial infarction (MI) as assessed by repeated angiographic examination. As can be observed from the figure, lesions that are non-significant (<50% stenosis) on prior angiography are frequently the underlying cause of MI. Moreover, non-significant lesions outnumber the more severely obstructive lesions and therefore account for the majority of MI. The bar charts were constructed from data published by Ambrose et al,⁹ Little et al,⁹⁶ Nobuyoshi et al,⁹⁷ and Giroud et al.⁹⁸

placement and pulsation.¹² Furthermore, reconstruction of 3-dimensional images from 2-dimensional projections using specially developed dedicated software may further enhance the angiographic assessment of coronary arteries (Figure 3). However, whether this novel technique will allow more accurate evaluation of atherosclerotic plaques remains to be determined more precisely.¹³ Overall, it seems evident that invasive coronary angiography is an excellent modality for detecting obstructive coronary artery disease. However, detailed imaging of atherosclerosis, such as determining the presence of vulnerable plaque characteristics, remodeling and inflammation, is still not feasible using this technique. Therefore other, more insightful modalities are needed for this purpose.

Intravascular ultrasound

With respect to the imaging of atherosclerosis, substantial progress has been achieved with the development of intravascular ultrasound (IVUS). IVUS is a minimally invasive imaging modality that uses miniaturized crystals incorporated at the catheter tip to provide real-time, high-resolution, cross-sectional images of the arterial wall and lumen. Axial resolution is approximately 150 μm and the lateral resolution 300 μm. As a result, the technique provides high-resolution images of the atherosclerotic process in the arterial wall.

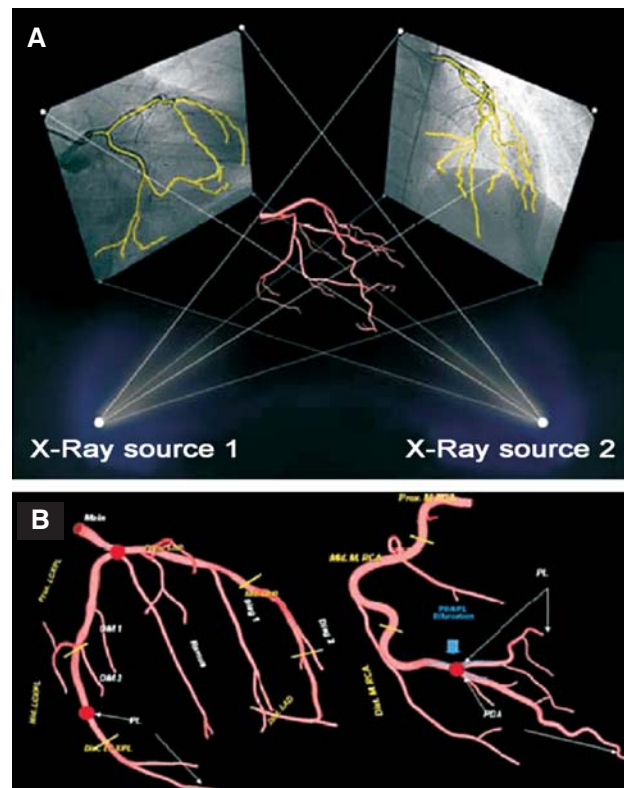


Figure 3. A: Illustration of three-dimensional coronary modeling based on two angiograms acquired in two different projection geometries. B: Modified American Heart Association (AHA) classification of coronary segments. Reprinted with permission from Garcia et al.⁹⁹

Importantly, the technique has been extensively validated against histological autopsy specimens of human coronary arteries.¹⁴⁻¹⁷ Both lumen and vessel dimensions, such as plaque and vessel area, plaque distribution, lesion length and remodeling index, can be accurately determined *in vivo*. In addition, semi-quantitative tissue characterization can be achieved based on plaque echogenicity. In conventional grayscale ultrasound images, calcium highly reflects ultrasound and appears as a bright and homogenous signal, resulting in acoustic shadowing.^{15,18} In addition, the severity of calcifications can be quantified by measuring the angle or arc of calcium. Hypo-echoic or low reflectance in IVUS images are usually due to lipid-laden lesions (also referred to as “soft” or “sonolucent” plaques). An example is provided in Figure 4.

Grayscale IVUS features of potentially vulnerable plaques have been evaluated prospectively by Yamagishi et al.¹⁹ The investigators evaluated 114 coronary plaques without luminal obstruction and assessed which plaques were related to an acute coronary event during a follow-up period of 21 months. Interestingly, it was reported that large, eccentric, positive remodeled plaques with an echolucent zone were at increased risk of instability (Figure 5). In addition, several retrospective studies confirmed that IVUS was able to identify plaques at higher risk of rupture (large echolucent area, thin fibrous cap).²⁰⁻²² Moreover, studies examining the differences between ruptured plaques and non-ruptured plaques in the same coronary artery demonstrated that the IVUS-derived lumen eccentricity index of ruptured plaques was greater.²³

IVUS has also been increasingly used as the gold standard in trials evaluating progression or regression of plaque in the coronary arteries. Indeed, unlike angiography, accurate quantification of plaque volume and area is provided by IVUS. Von Birgelen and co-workers performed IVUS examination of the left main coronary artery in 56 patients during initial angiography and repeated imaging after 18 months.²⁴ Adverse cardiovascular events occurred in 18 patients during follow up; in patients with events, annual plaque progression was significantly greater than in the remaining asymptomatic patients. Hence, it seems feasible that IVUS-measured progression of coronary plaque may serve as a marker for future cardiovascular events.

Nevertheless, the main limitation of grayscale IVUS remains its inability to accurately differentiate plaque composition. In particular, areas with low echo reflectance, such as fibrous tissue, fibro-fatty tissue and thrombus, remain hard to distinguish.^{14,18} More recently, integrated backscatter IVUS (IB-IVUS) systems have been developed to overcome this problem. Using this technique, a 2-dimensional color-coded map is constructed to reflect the tissue characteristics of the coronary arterial wall. In a prospective study by Sano et al, tissue characteristics of vulnerable plaques in patients prior to presentation with ACS were evaluated using IB-IVUS.²⁵ The authors demonstrated that the tissue characteristics of vulnerable plaques before they caused an ACS were different from those of plaques related to stable angina. However, a low positive predictive value of only 42% was reported for the identification of lipid area, indicating that further

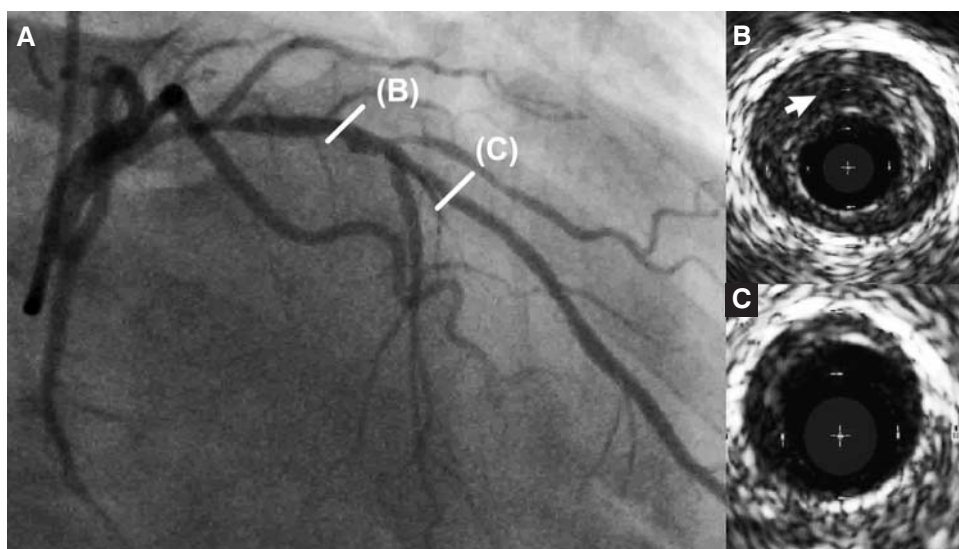


Figure 4. Coronary angiogram (A) of the left anterior descending coronary artery and corresponding intravascular ultrasound (IVUS) images (B and C) of a 55-year-old patient presenting with an acute coronary syndrome. In panel B an IVUS frame is provided showing a large plaque area with an echolucent zone (arrowhead) and luminal obstruction, possibly suggesting the presence of a vulnerable plaque. Panel C shows a more distally obtained IVUS frame with minimal plaque burden.

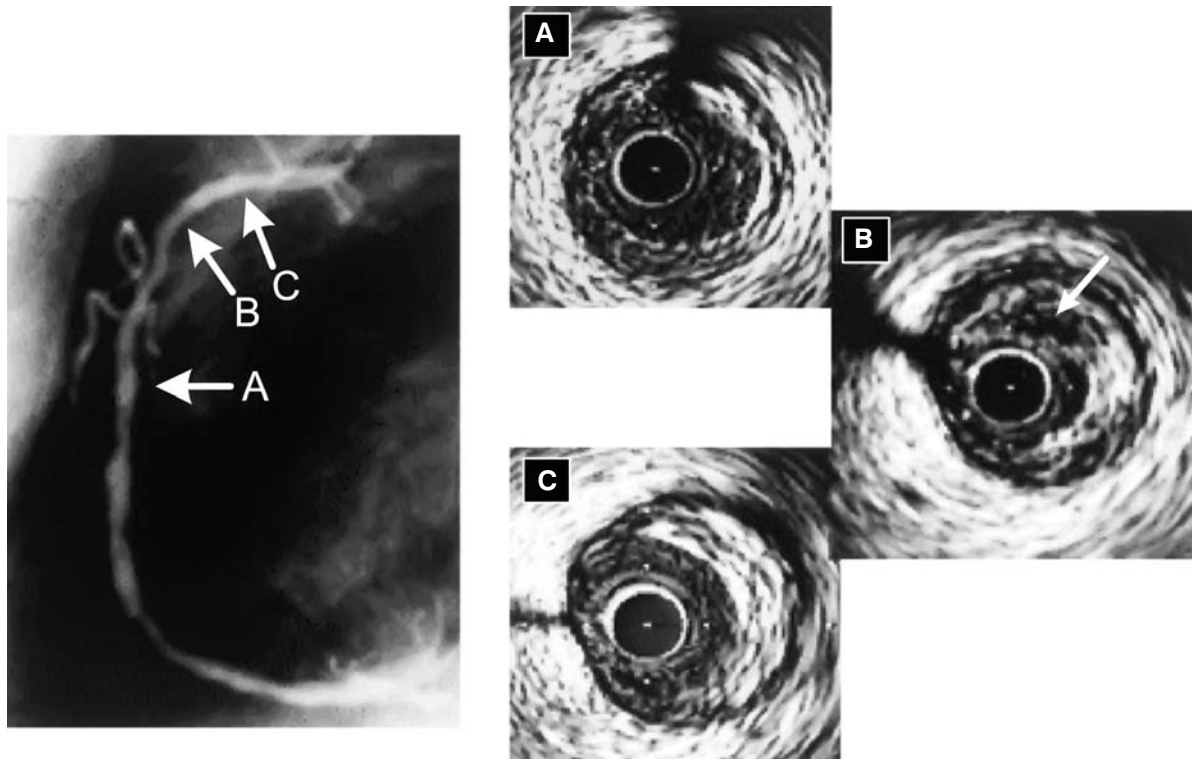


Figure 5. Coronary plaque in the right coronary artery (RCA) of a patient presenting with an acute coronary syndrome as evaluated by coronary angiography (left) and intravascular ultrasound (right). A: A mild concentric lesion in the distal part of the RCA. B: In the proximal portion, a significant eccentric lesion with an echolucent area (arrow) and high plaque burden of 67%. C: More proximally, an eccentric lesion with high echo density. Reprinted with permission from Yamagishi et al.¹⁹

improvement is needed before application of this technique is feasible.

Virtual histology intravascular ultrasound

Virtual histology intravascular ultrasound (VH IVUS) can potentially differentiate plaque composition more accurately than conventional grayscale IVUS. The technique is based on radiofrequency analysis of intravascular ultrasound backscatter signals. A combination of spectral parameters is used to develop statistical classification schemes for analysis of *in vivo* IVUS data in real time. Using these parameters, color-coded maps of plaque composition for each cross-sectional image are provided and are superimposed on the grayscale IVUS images. As illustrated in Figure 6, these tissue maps can differentiate fibrous (dark green), fibro-fatty (light green), dense calcium (white) and necrotic core (red) areas. Since its introduction, the technique has been validated by histology in several studies.^{26,27} Nair and colleagues have shown accuracies of 90.4% for fibrous,

92.8% for fibro-fatty, 90.9% for calcified and 89.5% for necrotic core regions, demonstrating the potential of this imaging tool for analyzing plaque composition.²⁶

The ability of VH IVUS to evaluate the presence of vulnerable plaques was first demonstrated by Rodriguez-Granillo et al.²⁸ The investigators observed that vulnerable plaques as determined on VH IVUS were more prevalent in patients presenting with ACS than in those with stable angina pectoris. Similar results were recently reported by Pundziute and co-workers, who demonstrated that in culprit lesions of patients with ACS the thin-capped fibroatheroma was more prevalent than in plaques of patients presenting with stable symptoms (Figure 7).²⁹ Interestingly, the presence of positive remodeling identified by VH IVUS was found to be similarly linked to the presence of vulnerable plaques. A retrospective study using VH IVUS demonstrated that positive remodeled plaque contained significantly more necrotic core and features of high-risk plaque, whereas negative remodeled plaques showed a more stable phenotype.³⁰

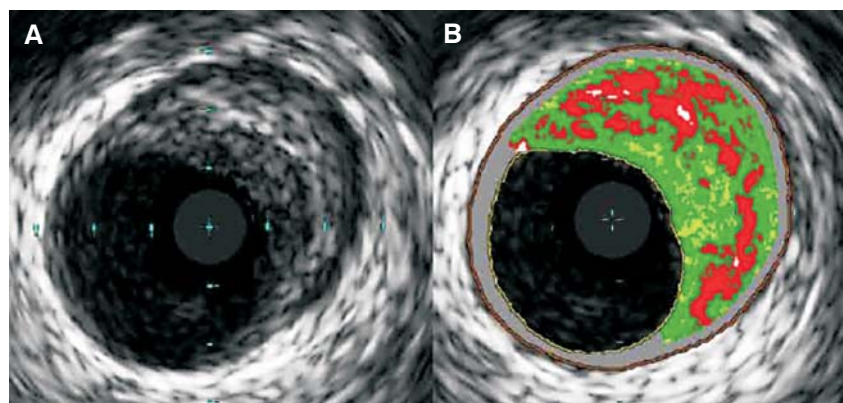


Figure 6. Plaque characterization by virtual histology intravascular ultrasound (VH IVUS). A: Traditional grayscale intravascular ultrasound (IVUS) frame showing coronary plaque. B: Example of VH IVUS color-coded map superimposed on grayscale IVUS frame. The colors correspond to different tissue types, such as fibrous (dark green), fibro-fatty (light green), dense calcium (white) and necrotic core (red). Panel B shows a plaque with predominantly necrotic core, small dense calcium deposits and a thick fibrous cap, corresponding to a fibroatheroma.

Notably, in addition to remodeling, Valgimigli et al demonstrated that plaque composition on VH IVUS was influenced by the location of the plaque in the coronary artery tree.³¹ As shown by VH IVUS, proximal segments of coronary arteries had a larger necrotic core area when compared to distal coronary segments, whereas the other plaque components (fibrous, fibro-fatty and dense calcium) were distributed evenly along the coronary artery tree. Accordingly, the distance from the ostium was demonstrated to be inversely associated with plaque vulnerability, possibly explaining

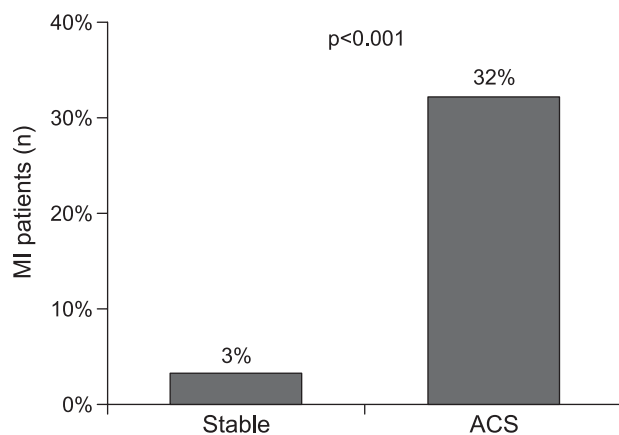


Figure 7. The prevalence of thin-capped fibroatheroma (TCFA) in patients presenting with stable symptoms versus patients presenting with an acute coronary syndrome (ACS) evaluated by virtual histology intravascular ultrasound. TCFAs were more frequently observed in plaques of patients with ACS (32%) as compared to patients with stable symptoms (3%). The bar chart was constructed with data from Pundziute et al.²⁹

the higher incidence of culprit lesions in proximal parts of the coronary artery tree.

Interestingly, in addition to evaluating progression or regression in plaque burden, VH IVUS may also have the ability to monitor changes in plaque composition (and possibly even plaque vulnerability) after treatment with anti-atherosclerotic therapy. Seruys et al assessed the effect of the direct lipoprotein-associated phospholipase A2 (Lp-PLA2) inhibitor darapladib on plaque composition by VH IVUS.³² The investigators showed that necrotic core size increased in patients receiving placebo. In contrast, Lp-PLA2 inhibition prevented further progression of necrotic core, suggesting stabilization of atherosclerosis.

Although VH IVUS is a promising imaging modality for plaque characterization, some limitations remain. Importantly, detection of the thin fibrous cap ($< 65 \mu\text{m}$) is not yet feasible as VH IVUS has a limited radial resolution of only $100 \mu\text{m}$. However, with the introduction of 40 MHz catheters imaging of the thin fibrous cap may eventually become possible.

Optical coherence tomography

Optical coherence tomography (OCT) is a unique high-resolution imaging technique that uses low coherence, near infrared light for intravascular imaging of the coronary artery wall. It has an excellent spatial resolution of $10\text{--}20 \mu\text{m}$, which is ten times higher than the resolution of IVUS. Furthermore, using histological controls, it has been demonstrated that OCT is su-

perior to IVUS in detecting important features of vulnerable plaque components, including thickness of fibrous cap, thrombus and density of macrophages.³³⁻³⁵

One of the first investigations to demonstrate the feasibility of plaque characterization with OCT *in vivo* was performed by Jang et al.³⁶ Using this technique the authors reported a higher frequency of thin-capped fibroatheroma in patients with ACS as compared to patients with stable angina pectoris. Kubo et al compared the assessment of culprit plaque morphology by OCT to grayscale IVUS and coronary angiography.³⁷ The authors concluded that OCT was superior in identifying the thin-capped fibroatheroma and thrombus, and that OCT was the only modality that could distinguish the thickness of the fibrous cap (Figure 8).

Another interesting feature of OCT is that it enables quantification of macrophages within fibrous caps. Tearney and colleagues showed *in vitro*, by comparing OCT images to histological specimens, that a high positive correlation exists between OCT measurements and fibrous cap macrophage density ($r=0.84$).³⁸ *In vivo*, Raffel and colleagues demonstrated a significant relationship between systemic inflammation (white cell blood count) and macrophage density in fibrous caps identified by OCT.³⁹

At present, it is important to realize that there are some important limitations in the use of OCT. Blood leads to significant attenuation of the emitted infrared light, therefore regular saline flushes or balloon occlusion of the artery is necessary for adequate imaging. Consequently, data acquisition is time-consuming and is therefore limited to focal lesion exploration. Furthermore, the penetration depth of near

infrared light is only 1-2 mm. As a result, OCT is not able to visualize the complete plaque and vessel wall, and quantitative measurements of plaque and/or lipid volume are currently not possible. However, a second-generation OCT technology, namely optical frequency domain imaging (OFDI), has recently been developed to enable imaging of the coronary arteries with a short, non-occlusive saline flush and rapid spiral pullback.⁴⁰

Other intracoronary techniques

Intravascular ultrasound palpography

Intravascular palpography is a technique based on intravascular ultrasound. This imaging modality allows the assessment of local mechanical tissue properties by assessing tissue deformation or strain. At a given pressure limit, fatty tissue components will show more deformation than fibrous components. Accordingly, palpography uses these differences in tissue deformation to differentiate between various plaque components. Indeed, differences in strain between fibrous, fibro-fatty and fatty components of the plaque of coronary and femoral arteries have been reported *in vitro*.⁴¹ In addition, a distinctive strain pattern was found with a high sensitivity and specificity (89%) for the detection of thin-capped fibroatheroma in post-mortem coronary arteries. Schaar et al performed the first clinical study using palpography in patients to assess the incidence of vulnerable plaque.⁴² In 55 patients presenting with stable symptoms, unstable symptoms and acute myocardial infarction, palpography was performed and the number of deformable pla-

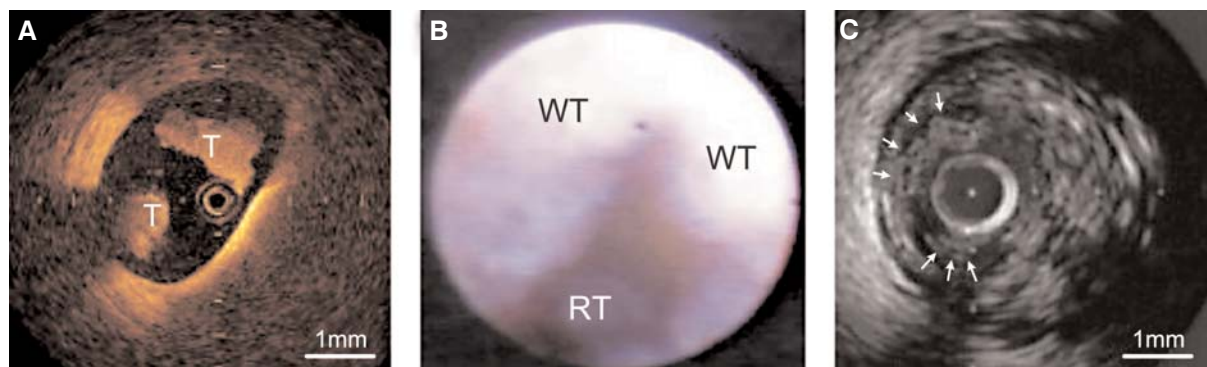


Figure 8. Intraluminal thrombi in corresponding images of optical coherence tomography (A), coronary angiography (B), and intravascular ultrasound (C). A: Thrombus with optical coherence tomography signal attenuation (T). B: Large white thrombus (WT) and small red thrombus (RT) adhering to a rough surface of yellow plaque. C: Thrombus (arrows) identified as a mass protruding into the vessel lumen from the surface of the vessel wall. Reprinted with permission from Kubo et al.³⁷

ques was assessed. The investigators reported that patients with stable angina pectoris had significantly fewer deformable plaques (high strain spots) per vessel as compared to patients presenting with unstable angina pectoris or acute myocardial infarction (Figure 9). Thus, although additional validation is required, intravascular ultrasound palpography appears to have potential for the identification of vulnerable plaque characteristics.

Intracoronary angiography

Intracoronary angiography is an imaging technique that uses optical fibers to allow direct visualization of the plaque surface, the presence of thrombus and the color of the luminal surface. A normal artery appears as glistening white, whereas a plaque can be categorized based on its angioscopic color, such as yellow or white. Additionally, thrombus can be identified as white (platelet rich) or red (platelets and erythrocytes) (Figure 8B). Uchida and co-workers performed intracoronary angiography in 157 patients presenting with stable angina.⁴³ In a 12-month follow-up period, ACS occurred more frequently in patients with glistening yellow plaques (69%) than in those with white plaques (3%).

Intracoronary angiography can also be applied as a tool for monitoring changes in plaque morphology

following pharmaceutical therapy. Using this technique, Takano and colleagues were able to demonstrate an effect of preventive treatment with atorvastatin.⁴⁴ Interestingly, lipid-lowering therapy with atorvastatin changed plaque color and morphology as determined by angiography, thereby suggesting plaque stabilization.

A major limitation of angiography remains that, as with OCT, the technique requires a blood-free field, while investigation is restricted to a limited part of the vessel.

Noninvasive imaging of atherosclerotic plaques

Calcium score

It has been well established that the presence of coronary artery calcifications (CAC) confirms the presence of atherosclerosis. In fact, an association between visible CAC on invasive coronary angiography and the risk of cardiovascular events was demonstrated in the early 1980s.⁴⁵ The introduction of electron beam computed tomography (EBCT) allowed the noninvasive evaluation of CAC and resulted in the development of the widely established quantification method by Agatston.⁴⁶ More recently, assessment of CAC is performed by means of multislice computed tomography (MSCT) (Figure 10).

The relation between the presence and extent of CAC and the presence of coronary artery stenosis has been assessed in several studies.⁴⁷⁻⁴⁹ As expected, a high sensitivity of CAC for the presence of obstructive CAD has been reported. However, extensive calcifications can be present in the absence of luminal narrowing. As a result, the specificity for obstructive CAD is low. Accordingly, the technique may be more suited to provide an estimate of total plaque burden rather than stenosis severity.

Importantly, data concerning the calcified plaque burden have been shown to translate into prognostic information. Indeed, the value of CAC scoring for risk stratification has been extensively studied. A large clinical trial by Greenland and colleagues showed the distinct incremental value of CAC scoring over the Framingham risk score in asymptomatic patients.⁵⁰ In addition, Detrano et al demonstrated that CAC performed equally well among the four major racial and ethnic groups.⁵¹ In a even larger cohort of 25,253 asymptomatic individuals, Budoff and colleagues confirmed that CAC was an independent predictor of mortality and that risk scores increased proportionally with higher

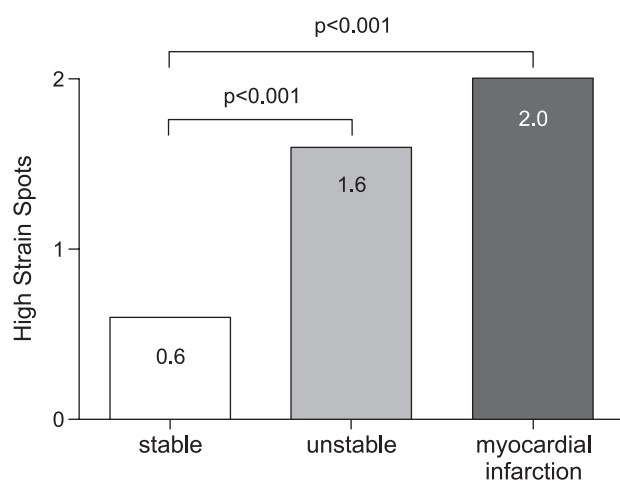


Figure 9. Bar chart representing the relation between the number of high strain spots as assessed by palpography and clinical presentation in 55 patients. High strain spots correspond to the more vulnerable plaques. More high strain spots were demonstrated by palpography in patients presenting with unstable angina pectoris and acute myocardial infarction as compared to patients presenting with stable angina pectoris. Bar chart constructed with data from Schaar et al.⁴²

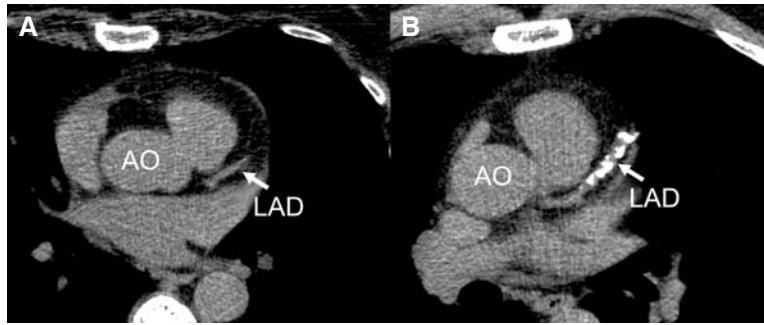


Figure 10. Example of coronary calcium on non-contrast-enhanced multislice computed tomography (MSCT) axial images. Calcifications appear as bright white dense structures on MSCT. Panel A shows a 57-year-old patient without evidence of coronary calcifications in the left anterior descending coronary artery (LAD). Panel B shows a 53-year-old patient with calcifications in the LAD. AO – aorta.

CAC scores (Figure 11).⁵² Particularly in patients initially classified as being at intermediate risk, knowledge of the extent of CAC may be valuable for refining risk stratification and determining further management.

In addition to risk stratification, it has been suggested that CAC scoring may allow noninvasive monitoring of changes in atherosclerotic plaque burden. Several investigations have demonstrated a halt in progression or even regression of coronary calcifications as a result of reductions in serum low-density lipoprotein (LDL) cholesterol concentrations.⁵³ However, other investiga-

tions failed to show such an effect, despite effective reductions in systemic inflammation or LDL cholesterol concentrations. It is possible that changes in calcified plaque burden may not adequately reflect changes in total atherosclerotic plaque burden. Moreover, it has been suggested that plaque stabilization may even be associated with a relative increase of coronary calcifications rather than a decrease. Indeed, it is important to realize that the presence or absence of calcium itself is not a direct marker for vulnerability. Since no information is obtained about the presence of non-calcified

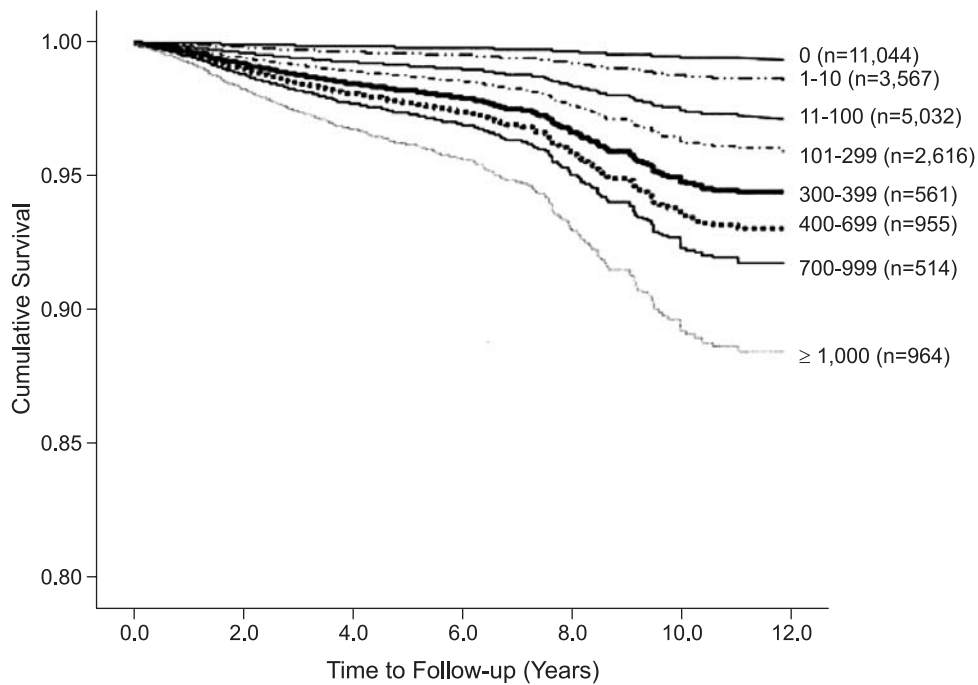


Figure 11. Cumulative survival by coronary artery calcification score, adjusted for risk factors such as age, hypercholesterolemia, diabetes, smoking, hypertension, and a family history of premature coronary artery disease. Increasing calcium scores were associated with worse survival and each increment of calcium score was associated with significant increased risk of all-cause mortality. Reprinted with permission from Budoff et al.⁵²

plaques, CAC scoring does not allow for a reliable distinction between potentially unstable versus stable plaques.⁵⁴

Multislice computed tomography angiography

MSCT is a rapidly evolving imaging tool that allows the noninvasive visualization of coronary atherosclerosis. Since the introduction of 4-slice scanners, the technique has developed rapidly and 64-slice and even 320-slice systems are currently available. The temporal and spatial resolution have improved accordingly, resulting in superior image quality and diagnostic accuracy for the detection of CAD. Although the resolution of MSCT remains inferior to that of invasive coronary angiography, high diagnostic accuracies have been demonstrated for the detection of significant CAD.⁵⁵ Additionally, the technique may be of use in the workup of patients presenting to the emergency department with suspected ACS. Promising results were reported by Hoffmann and co-workers, who demonstrated that the absence of significant coronary artery stenosis (73 of 103 patients) and non-significant coronary atherosclerotic plaque (41 of 103 patients) on MSCT accurately ruled out ACS.⁵⁶ Thus, a high negative predictive value was observed, indicating that MSCT angiography may be a valuable gatekeeper for invasive coronary angiography.

MSCT is not only able to identify coronary artery stenosis, but also has the potential to provide information about lesion morphology and plaque composition. As illustrated in Figure 12, the technique can distinguish non-calcified, mixed and calcified plaques. Due to the substantially higher density values, identification of calcified plaque is relatively simple on MSCT. However, identification of non-calcified plaque is more demanding because of the more subtle difference in attenuation and relatively larger influence of body-mass index, cardiac output and amount of contrast injected. Interestingly, a comparison between density measurements of non-calcified plaques on MSCT and invasive IVUS showed that the attenuation within hyper-echoic (fibrous) plaques was higher than within hypo-echoic (lipid-rich) plaques (mean attenuation values of 121 ± 34 HU versus 58 ± 43 HU).⁵⁷ However, for individual lesions a substantial overlap between hyper-echoic and hypo-echoic attenuation values was observed, indicating that at this stage further characterization of non-calcified plaque is not feasible.

Plaque composition as evaluated by MSCT has been linked to clinical presentation. Motoyama and col-

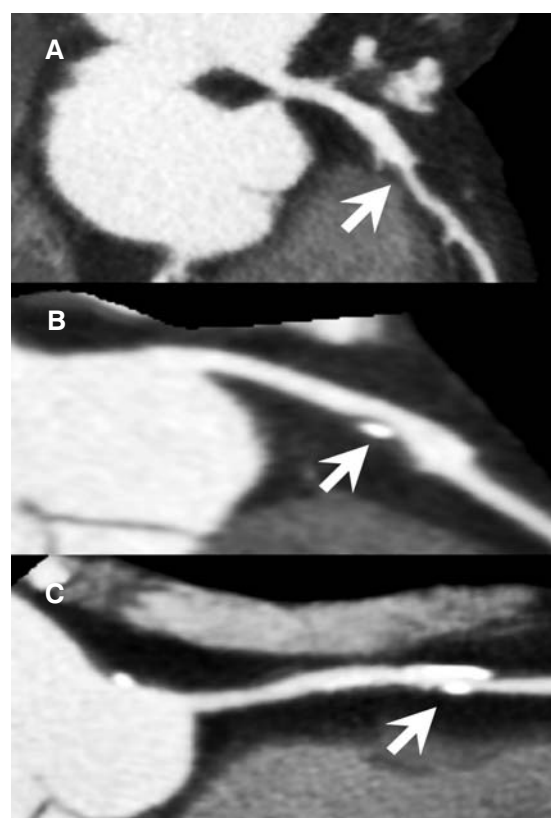


Figure 12. Example of plaque imaging performed on 320-slice multislice computed tomography coronary angiography. A: Curved multiplanar reconstruction of the left anterior descending artery (LAD) with non-calcified plaque (arrow). B: Curved multiplanar reconstruction of the LAD demonstrating mixed plaque (arrow). C: Curved multiplanar reconstruction of the right coronary artery demonstrating calcified plaque (arrow).

leagues compared plaque morphology on MSCT in 38 patients with ACS versus 33 patients with stable angina pectoris and demonstrated that plaques associated with ACS showed lower density values, positive remodeling and spotty calcification.⁵⁸ Pundziute and colleagues compared plaque characteristics on 64-slice MSCT and VH IVUS in patients with ACS and stable angina pectoris and demonstrated that non-calcified (32%) and mixed plaques (59%) were more frequently present in ACS.²⁹ In line with these findings, using 64-slice MSCT, Henneman et al demonstrated in 40 patients suspected of ACS that CAC was absent in a large proportion of patients (33%). However, as illustrated in Figure 13, in these patients non-calcified plaques were highly prevalent (39%).⁵⁹ As a result, atherosclerosis and even obstructive CAD were frequently observed, even in the absence of detectable calcium. Thus, the investigators suggested that in patients presenting with

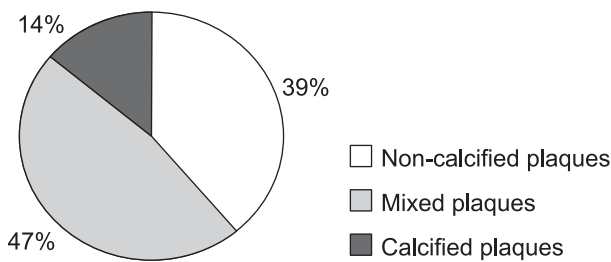


Figure 13. Prevalence of different plaque types in patients presenting with suspected acute coronary syndrome (ACS). A high prevalence of non-calcified and mixed plaques was observed in patients presenting with suspected ACS. Pie chart constructed with data from Henneman et al.⁵⁹

ACS, the absence of CAC does not reliably exclude CAD.

Preliminary studies have suggested that information about atherosclerosis derived from MSCT angiography may also provide prognostic information.^{60,61} Interestingly, van Werkhoven et al demonstrated that the presence of a substantial non-calcified plaque burden was an independent predictor of events (all-cause mortality, non-fatal myocardial infarction, and unstable angina requiring revascularization).⁶² However, further investigations are required in larger patient populations to confirm these observations.

In addition, MSCT may potentially be applied to monitor the progression and/or regression of coronary plaque burden. Preliminary results from an experimental animal model indicated that MSCT could accurately document serial changes in aortic plaque burden that correlated well with measurements derived from magnetic resonance imaging (MRI).⁶³ In humans, Burgstahler and co-workers studied the effect of lipid-lowering therapy on coronary plaque burden with MSCT after one year.⁶⁴ Although no differences were found in total plaque burden and CAC, a significantly lower non-calcified plaque burden was demonstrated after lipid-lowering therapy.

While MSCT angiography may have potential for the noninvasive evaluation of plaque composition and subsequent identification of patients at higher risk of events, several important limitations remain. Firstly, the technique is associated with radiation exposure, although significant dose reductions have been achieved with recent advances in scanner hardware and acquisition protocols.⁶⁵⁻⁶⁷ In addition, the resolution remains inferior compared to invasive atherosclerosis imaging techniques and no validated algorithms are currently available for the quantification of observations. Further improvement in plaque characterization, however, is expected with the development of dual-energy MSCT or dedicated contrast agents.

Magnetic resonance imaging

MRI is a versatile imaging technique with a high potential to visualize vessel anatomy. The technique is able to differentiate atherosclerotic tissue without exposure to radiation, using features such as chemical composition, water content, molecular motion, or diffusion. Due to recent improvements in MR techniques, such as high-resolution and multi-contrast MR – T1- and T2-weighted, proton density (PD) weighted and time-of-flight (TOF) imaging – plaque characterization has become possible, as demonstrated in experimental models, histological specimens, human carotid arteries and the aortic wall *in vivo* (Table 2).⁶⁸⁻⁷¹ Fayad and colleagues assessed aortic wall plaque composition with MR images matched to transesophageal echocardiograms, demonstrating a strong correlation for plaque composition, thickness and extent.⁶⁸ In several studies, the potential of MRI to characterize different plaque characteristics, including the fibrous cap, lipid core and even the presence of hemorrhage in human carotid atherosclerotic plaques (Figure 14), has been demonstrated.^{72,73} In addition, a good correlation has been identified between fibrous cap integrity on MRI and histopathological specimens.⁶⁹

Table 2. Multicontrast weightings and corresponding plaque characterization on magnetic resonance imaging. Intensities are relative to that of the sternomastoid muscle. Table modified from Yuan et al.⁹⁴

Component	TOF	T1-weighted	T2-weighted	PD-weighted
Hemorrhage	High	High - moderate	Variable	Variable
Lipid-rich necrotic core	Moderate	High	Variable	High
Calcification	Low	Low	Low	Low
Fibrous tissue	Moderate - low	Moderate	Variable	High

TOF - time of flight; PD - proton density.

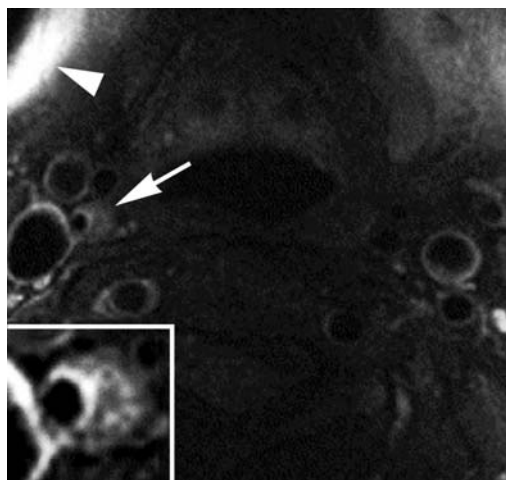


Figure 14. Example of magnetic resonance image (T2-weighted) of the carotid arteries. A stenotic lesion of the right internal carotid artery can be observed just distal to the bifurcation (arrow). The arrowhead indicates a high signal artifact from the closely placed superficial phase-array coil. Finally, in the enlargement, a hypo-intense signal within the plaque, corresponding to lipid accumulation, can be observed. Reprinted with permission from Corti et al.¹⁰⁰

Plaque imaging of the coronary arteries with MRI remains challenging, since deep location, motion and respiratory artifacts, and small caliber vessels remain obstacles for accurate coronary visualization and plaque differentiation. Nevertheless, several novel approaches for coronary plaque imaging are currently under development and may potentially allow accurate evaluation of atherosclerotic plaque in the coronary arteries.⁷⁴ In particular “black-blood” techniques (an imaging approach in which the blood appears black and the arterial wall can be seen) are promising for accurately portraying plaque presence, size and morphology with sub-millimeter resolution and high reproducibility.⁷⁵ Kim et al recently applied a novel 3-dimensional free breathing black-blood fast gradient technique with real-time motion correction developed by Botnar et al to evaluate patients with non-significant CAD and compared these patients to a control group without CAD.^{76,77} The investigators demonstrated that MRI could identify significantly increased vessel wall thickness with preserved lumen size in patients with non-significant CAD.

High-resolution MRI, in combination with molecular contrast agents targeted to specific cells or molecules, offers an interesting alternative approach for more detailed plaque characterization.⁷⁸⁻⁸⁰ In particular, contrast agents dedicated to the identification of vulnerable plaque components are of considerable interest. Paramagnetic contrast agents such as gado-

linium (T₁-shortening contrast with a high affinity for lipid-rich lesions) are able to assess the more subtle differences in plaque composition.⁷⁹ Furthermore, T₂-shortening contrast agents such as ultra small superparamagnetic particles of iron oxide (USPIOs) have been studied both *in vitro* and *in vivo*. Interestingly, these particles were found to accumulate in plaques with a high macrophage content and caused a signal decrease in MR images.⁸¹ Additionally, promising results have been achieved with fibrin-targeted contrast agents, which have the potential to allow noninvasive molecular imaging of thrombus. Spuentrup and colleagues demonstrated in an experimental animal model that, using these agents, acute pulmonary, cardiac and coronary thrombosis could be accurately visualized by MR imaging.⁸² Furthermore, continued advances in radiofrequency hardware have resulted in an increase in the operating field strength from 1.5 T (tesla) to 3 T and even 7 T. At 3 T an approximately twofold increase in signal-to-noise ratio can be obtained, resulting in a fourfold reduction in scanning time and a significant increase in temporal resolution.

Recent studies also support MRI as an effective tool to evaluate plaque regression following lipid-lowering therapy. Corti et al demonstrated in 18 hypercholesterolemic patients that MRI could document a marked reduction in atherosclerotic lesion size induced by statin therapy in humans.⁸³ Accordingly, MRI may become a particular attractive modality for the noninvasive monitoring of the effect of anti-atherosclerotic interventions *in vivo*.

Nevertheless, detailed characterization of plaque, including the identification of high-risk features, remains difficult at present. Although much is expected from current developments, evidently more data are needed before plaque characterization with MRI may be used clinically for the identification and management of patients at risk.

Molecular imaging with nuclear techniques

Using dedicated tracers, nuclear imaging techniques such as single photon emission tomography (SPECT) and positron emission tomography (PET) can target distinct mediators and regulators involved in the cascade of atherosclerosis. As a result of increasing knowledge regarding the pathophysiology of atherosclerosis, several radionuclide-labeled tracers that serve as markers of inflammation, angiogenesis, apoptosis and lipid metabolism have been developed for plaque imaging (Table 3).

Table 3. Targets for molecular imaging of plaque vulnerability. Table modified from Narula et al.⁹⁵

Process targeted	Targets	Target agents
Monocyte migration:		
Reversible prelude with intima	Selectins	Microbubbles with antibodies
Receptors for chemotactic peptides	MCP-1	Radiolabeled MCP-1
Activation-dependent receptors	ICAM or VCAM	Antibodies; radiolabeled or on microbubbles
Subintimal activation of monocytes:		
Lipid scavenging receptors	SRA I,II	Oxidized LDL
Other phagocyte receptors	FcγRIII	Radiolabeled non-specific IgG or Fc fragments
Immune activation	PS receptor	PS-rich microbubbles
Heightened metabolic activity	Others	Superparamagnetic iron (USPIOs); nanoparticulate CT contrast
	HLA expression	Radiolabeled antibody
	FDG	Positron-labeled FDG
Macrophage apoptosis:		
Cell membrane	PS expression	Radiolabeled Annexin A5
Cell apoptosis pathways	Caspase substrate	Radiolabeled DEVD
Collateral products from macrophages:		
Cytokines	MMPs	MMP inhibitor or substrate; radiolabeled or fluorochromes
<i>Vasa vasorum</i> or neovascularization	Integrins	Radiolabeled RDG peptide
	VEGF	Radiolabeled VEGF

FDG – fluorodeoxyglucose; HLA – human leukocyte antigen; ICAM – intercellular adhesion molecule; MCP-1 – monocyte chemoattractant protein 1; MMP – matrix metalloproteinase; PS – phosphatidylserine; SRA – scavenger receptor A; VCAM – vascular cell adhesion molecule; VEGF – vascular endothelial growth factor.

Matrix metalloproteinases (MMP) are released by activated macrophages and are therefore used to identify proteolytic activity in atherosclerotic lesions. MMPs modulate the degrading of the extracellular matrix and the thin fibrous cap of an atherosclerotic lesion, contributing to the vulnerability of the plaque. The feasibility of *in vivo* imaging of MMP activity using radionuclide-labeled MMP inhibitors has been shown in several animal models.⁸⁴⁻⁸⁶

Additionally, it has been proposed that apoptosis is one of the features of an atherosclerotic unstable lesion and that apoptosis consequently leads to growth of the necrotic core and influences plaque stability. Annexin A5 has a high affinity for phosphatidylserine (exposed on the plasma membrane of apoptotic cells) and therefore radionuclide-labeled Annexin A5 can be used as a marker of apoptotic cells in atherosclerotic lesions. In experimental models, a direct correlation was demonstrated between Annexin A5 uptake, macrophage burden and histologically demonstrated apoptosis.⁸⁷ In a small patient cohort with a history of transient ischemic attack, Annexin A5 imaging of carotid atherosclerosis was performed by Kietselaer et al.⁸⁸ Imaging was performed before carotid surgery and correlated with histopathology findings. The investigators reported that Annexin A5 uptake in carotid lesions correlated highly with plaque instability. However, only preliminary data are available and further research in humans is necessary.

Finally, PET imaging with F18-fluorodeoxyglucose (FDG) is currently considered to be one of the most promising imaging modalities for the identification of vulnerable lesions. FDG is a radionuclide trac-

er that competes with glucose for uptake into metabolically active cells, especially macrophages, and enables quantification via PET. Within carotid artery atherosclerotic plaques, Rudd et al demonstrated with FDG PET that FDG was taken up by resident macrophages in atherosclerotic plaque but not by surrounding cellular plaque components.⁸⁹ The authors suggested that FDG may be capable of imaging and possibly even quantification of plaque inflammation. In addition, FDG PET could potentially be used to serially monitor changes in atherosclerotic plaque macrophage content. In an experimental rabbit model, Worthley and co-workers demonstrated that assessment of progression and/or regression of macrophage content in atherosclerotic plaques was feasible using this noninvasive technique.⁹⁰ In addition, Tahara et al showed in 43 patients that FDG PET, co-registered with computed tomography data, was able to visualize significantly reduced plaque inflammation following 3 months' treatment with simvastatin.⁹¹

However, thus far FDG imaging of the coronary arteries has been challenging because of cardiac motion, FDG uptake in the myocardium, and the limited resolution of PET. Co-registration of the functional images with high-resolution anatomical data obtained with MSCT in combination with dedicated protocols to suppress myocardial uptake could possibly overcome this limitation (Figure 15).^{92,93}

Summary and conclusions

Plaque rupture followed by coronary occlusion due to thrombosis is responsible for a large number of acute

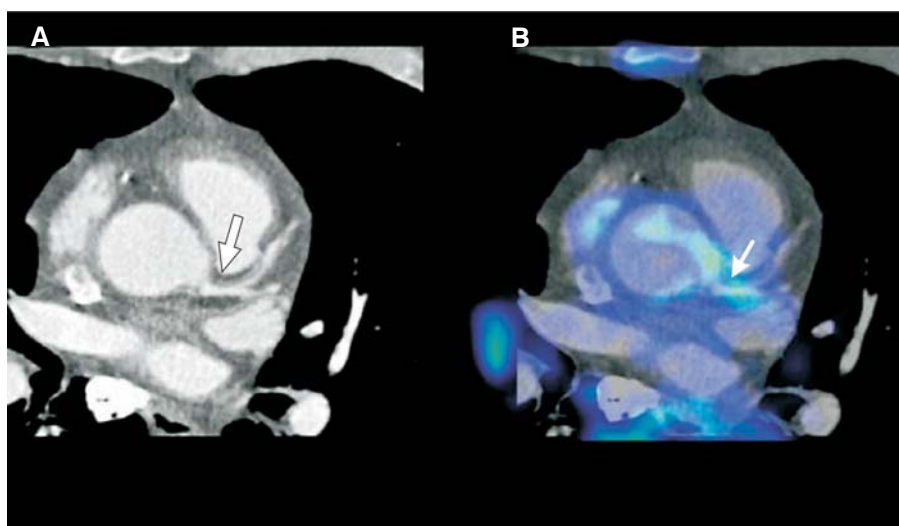


Figure 15. Example of the co-registration of functional imaging with F-18 fluorodeoxyglucose (FDG) positron emission tomography (PET) and anatomical imaging with multislice computed tomography (MSCT). A: On MSCT axial images a non-calcified plaque in the left main coronary artery (arrow) was identified. B: Corresponding image after fusion with F-18 FDG PET, localizing the inflammatory PET signal with a maximal standard uptake value of 2.1 to the non-calcified plaque seen in the left coronary artery (arrow). Reprinted with permission from Alexanderson et al.⁹²

coronary events. Identification of lesions before they rupture would allow the initiation of aggressive systemic or even local therapy and could potentially improve outcome. In the absence of natural history data, the precursor of vulnerable lesions remains largely unknown and most details have been derived from retrospective postmortem studies. On the basis of these investigations, it has been suggested that the most common substrate for superimposed thrombus formation is the thin-capped fibroatheroma, a plaque with a large necrotic core and an inflamed thin fibrous cap (<65 μm thick) infiltrated by macrophages and lymphocytes.

As discussed in the current review, extensive effort has been invested in the development of imaging tools to characterize coronary atherosclerosis, with the ultimate goal of detecting vulnerable lesions. To this end, several techniques are currently under investigation, with each technique having specific advantages as well as limitations. Importantly, the clinical relevance in terms of predicting outcome and changing management remains to be established for all currently available techniques.

At present, invasive techniques, such as OCT and VH IVUS, provide the most detailed information and are currently employed in prospective natural history studies. Given their invasive nature, the application of these techniques will remain largely restricted to symptomatic high-risk patients, whereas a noninvasive technique would allow application on a wider scale. At present, noninvasive approaches cannot provide detailed characterization of the individual vulnerable coronary plaque. However, direct *in vivo* comparisons with invasive modalities may substantially improve our understanding and interpretation of noninvasive observations. Consequently, this information may be translated into enhanced strategies for risk stratification. In addition, the measurements of plaque vulnerability obtained with either invasive or noninvasive imaging techniques may be used as a surrogate endpoint for prospective anti-atherosclerotic therapy trials.³² Possibly, the combination of imaging techniques targeting both morphological and functional characteristics may be of particular value.

Evidently, large prospective studies are needed to further define the potential role of each imaging technique in the identification of vulnerable plaques. Moreover, much uncertainty remains concerning how these vulnerable lesions should be treated. In addition to an increased intensity of systemic therapy, such as aspirin and statin therapy, local or regional

therapeutic approaches (such as plaque sealing) have also been suggested. However, no robust data are currently available to support their effectiveness. Potentially, imaging techniques may prove of great value in the development of such individually targeted treatment strategies.

References

1. Falk E, Shah PK, Fuster V. Coronary plaque disruption. *Circulation*. 1995; 92: 657-671.
2. van der Wal AC, Becker AE, van der Loos CM, Das PK. Site of intimal rupture or erosion of thrombosed coronary atherosclerotic plaques is characterized by an inflammatory process irrespective of the dominant plaque morphology. *Circulation*. 1994; 89: 36-44.
3. Virmani R, Kolodgie FD, Burke AP, Farb A, Schwartz SM. Lessons from sudden coronary death: a comprehensive morphological classification scheme for atherosclerotic lesions. *Arterioscler Thromb Vasc Biol*. 2000; 20: 1262-1275.
4. Schaar JA, Muller JE, Falk E, et al. Terminology for high-risk and vulnerable coronary artery plaques. Report of a meeting on the vulnerable plaque, June 17 and 18, 2003, Santorini, Greece. *Eur Heart J*. 2004; 25: 1077-1082.
5. Moreno PR, Falk E, Palacios IF, Newell JB, Fuster V, Fallon JT. Macrophage infiltration in acute coronary syndromes. Implications for plaque rupture. *Circulation*. 1994; 90: 775-778.
6. Gimbrone MA, Jr, Nagel T, Topper JN. Biomechanical activation: an emerging paradigm in endothelial adhesion biology. *J Clin Invest*. 1997; 99: 1809-1813.
7. Ross R. Atherosclerosis—an inflammatory disease. *N Engl J Med*. 1999; 340: 115-126.
8. Kunsch C, Medford RM. Oxidative stress as a regulator of gene expression in the vasculature. *Circ Res*. 1999; 85: 753-766.
9. Ambrose JA, Tannenbaum MA, Alexopoulos D, et al. Angiographic progression of coronary artery disease and the development of myocardial infarction. *J Am Coll Cardiol*. 1988; 12: 56-62.
10. White CW, Wright CB, Doty DB, et al. Does visual interpretation of the coronary arteriogram predict the physiologic importance of a coronary stenosis? *N Engl J Med*. 1984; 310: 819-824.
11. Garcia JA, Chen SY, Messenger JC, et al. Initial clinical experience of selective coronary angiography using one prolonged injection and a 180 degrees rotational trajectory. *Catheter Cardiovasc Interv*. 2007; 70: 190-196.
12. Maddux JT, Wink O, Messenger JC, et al. Randomized study of the safety and clinical utility of rotational angiography versus standard angiography in the diagnosis of coronary artery disease. *Catheter Cardiovasc Interv*. 2004; 62: 167-174.
13. Hoffmann KR, Wahle A, Pellot-Barakat C, Sklansky J, Sonka M. Biplane X-ray angiograms, intravascular ultrasound, and 3D visualization of coronary vessels. *Int J Card Imaging*. 1999; 15: 495-512.
14. Di Mario C, The SH, Madretsma S, et al. Detection and characterization of vascular lesions by intravascular ultrasound: an *in vitro* study correlated with histology. *J Am Soc Echocardiogr*. 1992; 5: 135-146.
15. Gussenhoven EJ, Essed CE, Lancee CT, et al. Arterial wall

- characteristics determined by intravascular ultrasound imaging: an in vitro study. *J Am Coll Cardiol.* 1989; 14: 947-952.
16. Kostamäa H, Donovan J, Kasaoka S, Tobis J, Fitzpatrick L. Calcified plaque cross-sectional area in human arteries: correlation between intravascular ultrasound and undecalcified histology. *Am Heart J.* 1999; 137: 482-488.
 17. Siegel RJ. Histopathologic validation of angiography and intravascular ultrasound. *Circulation.* 1991; 84: 109-117.
 18. Potkin BN, Bartorelli AL, Gessert JM, et al. Coronary artery imaging with intravascular high-frequency ultrasound. *Circulation.* 1990; 81: 1575-1585.
 19. Yamagishi M, Terashima M, Awano K, et al. Morphology of vulnerable coronary plaque: insights from follow-up of patients examined by intravascular ultrasound before an acute coronary syndrome. *J Am Coll Cardiol.* 2000; 35: 106-111.
 20. Ge J, Baumgart D, Haude M, et al. Role of intravascular ultrasound imaging in identifying vulnerable plaques. *Herz.* 1999; 24: 32-41.
 21. Kotani J, Mintz GS, Castagna MT, et al. Intravascular ultrasound analysis of infarct-related and non-infarct-related arteries in patients who presented with an acute myocardial infarction. *Circulation.* 2003; 107: 2889-2893.
 22. Rioufol G, Finet G, Ginon I, et al. Multiple atherosclerotic plaque rupture in acute coronary syndrome: a three-vessel intravascular ultrasound study. *Circulation.* 2002; 106: 804-808.
 23. von Birgelen C, Klinkhart W, Mintz GS, et al. Plaque distribution and vascular remodeling of ruptured and nonruptured coronary plaques in the same vessel: an intravascular ultrasound study in vivo. *J Am Coll Cardiol.* 2001; 37: 1864-1870.
 24. von Birgelen C, Hartmann M, Mintz GS, et al. Relationship between cardiovascular risk as predicted by established risk scores versus plaque progression as measured by serial intravascular ultrasound in left main coronary arteries. *Circulation.* 2004; 110: 1579-1585.
 25. Sano K, Kawasaki M, Ishihara Y, et al. Assessment of vulnerable plaques causing acute coronary syndrome using integrated backscatter intravascular ultrasound. *J Am Coll Cardiol.* 2006; 47: 734-741.
 26. Nair A, Kuban BD, Tuzcu EM, Schoenhagen P, Nissen SE, Vince DG. Coronary plaque classification with intravascular ultrasound radiofrequency data analysis. *Circulation.* 2002; 106: 2200-2206.
 27. Nasu K, Tsuchikane E, Katoh O, et al. Accuracy of in vivo coronary plaque morphology assessment: a validation study of in vivo virtual histology compared with in vitro histopathology. *J Am Coll Cardiol.* 2006; 47: 2405-2412.
 28. Rodriguez-Granillo GA, Garcia-Garcia HM, Mc Fadden EP, et al. In vivo intravascular ultrasound-derived thin-cap fibroatheroma detection using ultrasound radiofrequency data analysis. *J Am Coll Cardiol.* 2005; 46: 2038-2042.
 29. Pundziute G, Schuijff JD, Jukema JW, et al. Evaluation of plaque characteristics in acute coronary syndromes: non-invasive assessment with multi-slice computed tomography and invasive evaluation with intravascular ultrasound radiofrequency data analysis. *Eur Heart J.* 2008; 29: 2373-2381.
 30. Rodriguez-Granillo GA, Serruys PW, Garcia-Garcia HM, et al. Coronary artery remodelling is related to plaque composition. *Heart.* 2006; 92: 388-391.
 31. Valgimigli M, Rodriguez-Granillo GA, Garcia-Garcia HM, et al. Distance from the ostium as an independent determinant of coronary plaque composition in vivo: an intravascular ultrasound study based radiofrequency data analysis in humans. *Eur Heart J.* 2006; 27: 655-663.
 32. Serruys PW, Garcia-Garcia HM, Buszman P, et al. Effects of the direct lipoprotein-associated phospholipase A(2) inhibitor darapladib on human coronary atherosclerotic plaque. *Circulation.* 2008; 118: 1172-1182.
 33. Jang IK, Bouma BE, Kang DH, et al. Visualization of coronary atherosclerotic plaques in patients using optical coherence tomography: comparison with intravascular ultrasound. *J Am Coll Cardiol.* 2002; 39: 604-609.
 34. Tanaka A, Imanishi T, Kitabata H, et al. Distribution and frequency of thin-capped fibroatheromas and ruptured plaques in the entire culprit coronary artery in patients with acute coronary syndrome as determined by optical coherence tomography. *Am J Cardiol.* 2008; 102: 975-979.
 35. Yabushita H, Bouma BE, Houser SL, et al. Characterization of human atherosclerosis by optical coherence tomography. *Circulation.* 2002; 106: 1640-1645.
 36. Jang IK, Tearney GJ, MacNeill B, et al. In vivo characterization of coronary atherosclerotic plaque by use of optical coherence tomography. *Circulation.* 2005; 111: 1551-1555.
 37. Kubo T, Imanishi T, Takarada S, et al. Assessment of culprit lesion morphology in acute myocardial infarction: ability of optical coherence tomography compared with intravascular ultrasound and coronary angiography. *J Am Coll Cardiol.* 2007; 50: 933-939.
 38. Tearney GJ, Yabushita H, Houser SL, et al. Quantification of macrophage content in atherosclerotic plaques by optical coherence tomography. *Circulation.* 2003; 107: 113-119.
 39. Raffel OC, Tearney GJ, Gauthier DD, Halpern EF, Bouma BE, Jang IK. Relationship between a systemic inflammatory marker, plaque inflammation, and plaque characteristics determined by intravascular optical coherence tomography. *Arterioscler Thromb Vasc Biol.* 2007; 27: 1820-1827.
 40. Tearney GJ, Waxman S, Shishkov M, et al. Three-dimensional coronary artery microscopy by intracoronary optical frequency domain imaging. *JACC Cardiovasc Imaging.* 2008; 1: 752-761.
 41. de Korte CL, Pasterkamp G, van der Steen AF, Woutman HA, Bom N. Characterization of plaque components with intravascular ultrasound elastography in human femoral and coronary arteries in vitro. *Circulation.* 2000; 102: 617-623.
 42. Schaar JA, de Korte CL, Mastik F, et al. Characterizing vulnerable plaque features with intravascular elastography. *Circulation.* 2003; 108: 2636-2641.
 43. Uchida Y, Nakamura F, Tomaru T, et al. Prediction of acute coronary syndromes by percutaneous coronary angiography in patients with stable angina. *Am Heart J.* 1995; 130: 195-203.
 44. Takano M, Mizuno K, Yokoyama S, et al. Changes in coronary plaque color and morphology by lipid-lowering therapy with atorvastatin: serial evaluation by coronary angiography. *J Am Coll Cardiol.* 2003; 42: 680-686.
 45. Margolis JR, Chen JT, Kong Y, Peter RH, Behar VS, Kisslo JA. The diagnostic and prognostic significance of coronary artery calcification. A report of 800 cases. *Radiology.* 1980; 137: 609-616.
 46. Agatston AS, Janowitz WR, Hildner FJ, et al. Quantification of coronary artery calcium using ultrafast computed tomography. *J Am Coll Cardiol.* 1990; 15: 827-832.
 47. Budoff MJ, Diamond GA, Raggi P, et al. Continuous probabilistic prediction of angiographically significant coronary artery disease using electron beam tomography. *Circulation.* 2002; 105: 1791-1796.
 48. Haberl R, Becker A, Leber A, et al. Correlation of coronary calcification and angiographically documented stenoses in

- patients with suspected coronary artery disease: results of 1,764 patients. *J Am Coll Cardiol.* 2001; 37: 451-457.
49. Nallamothu BK, Saint S, Bielak LF, et al. Electron-beam computed tomography in the diagnosis of coronary artery disease: a meta-analysis. *Arch Intern Med.* 2001; 161: 833-838.
 50. Greenland P, LaBree L, Azen SP, Doherty TM, Detrano RC. Coronary artery calcium score combined with Framingham score for risk prediction in asymptomatic individuals. *JAMA.* 2004; 291: 210-215.
 51. Detrano R, Guerci AD, Carr JJ, et al. Coronary calcium as a predictor of coronary events in four racial or ethnic groups. *N Engl J Med.* 2008; 358: 1336-1345.
 52. Budoff MJ, Shaw LJ, Liu ST, et al. Long-term prognosis associated with coronary calcification: observations from a registry of 25,253 patients. *J Am Coll Cardiol.* 2007; 49: 1860-1870.
 53. Achenbach S, Ropers D, Pohle K, et al. Influence of lipid-lowering therapy on the progression of coronary artery calcification: a prospective evaluation. *Circulation.* 2002; 106: 1077-1082.
 54. Schmermund A, Erbel R. Unstable coronary plaque and its relation to coronary calcium. *Circulation.* 2001; 104: 1682-1687.
 55. Budoff MJ, Dowe D, Jollis JG, et al. Diagnostic performance of 64-multidetector row coronary computed tomographic angiography for evaluation of coronary artery stenosis in individuals without known coronary artery disease: results from the prospective multicenter ACCURACY (Assessment by Coronary Computed Tomographic Angiography of Individuals Undergoing Invasive Coronary Angiography) trial. *J Am Coll Cardiol.* 2008; 52: 1724-1732.
 56. Hoffmann U, Nagurney JT, Moselewski F, et al. Coronary multidetector computed tomography in the assessment of patients with acute chest pain. *Circulation.* 2006; 114: 2251-2260.
 57. Pohle K, Achenbach S, Macneill B, et al. Characterization of non-calcified coronary atherosclerotic plaque by multi-detector row CT: comparison to IVUS. *Atherosclerosis.* 2007; 190: 174-180.
 58. Motoyama S, Kondo T, Sarai M, et al. Multislice computed tomographic characteristics of coronary lesions in acute coronary syndromes. *J Am Coll Cardiol.* 2007; 50: 319-326.
 59. Henneman MM, Schuijf JD, Pundziute G, et al. Noninvasive evaluation with multislice computed tomography in suspected acute coronary syndrome: plaque morphology on multislice computed tomography versus coronary calcium score. *J Am Coll Cardiol.* 2008; 52: 216-222.
 60. Min JK, Shaw LJ, Devereux RB, et al. Prognostic value of multidetector coronary computed tomographic angiography for prediction of all-cause mortality. *J Am Coll Cardiol.* 2007; 50: 1161-1170.
 61. Pundziute G, Schuijf JD, Jukema JW, et al. Prognostic value of multislice computed tomography coronary angiography in patients with known or suspected coronary artery disease. *J Am Coll Cardiol.* 2007; 49: 62-70.
 62. van Werkhoven JM, Schuijf JD, Gaemperli O, et al. Prognostic value of multislice computed tomography and gated single-photon emission computed tomography in patients with suspected coronary artery disease. *J Am Coll Cardiol.* 2009; 53: 623-632.
 63. Ibanez B, Cimmino G, Benezet-Mazuecos J, et al. Quantification of serial changes in plaque burden using multi-detector computed tomography in experimental atherosclerosis. *Atherosclerosis.* 2009; 202: 185-191.
 64. Burgstahler C, Reimann A, Beck T, et al. Influence of a lipid-lowering therapy on calcified and noncalcified coronary plaques monitored by multislice detector computed tomography: results of the New Age II Pilot Study. *Invest Radiol.* 2007; 42: 189-195.
 65. Earls JP, Berman EL, Urban BA, et al. Prospectively gated transverse coronary CT angiography versus retrospectively gated helical technique: improved image quality and reduced radiation dose. *Radiology.* 2008; 246: 742-753.
 66. Husmann L, Valenta I, Gaemperli O, Adda O, Treyer V, Wyss C. Feasibility of low-dose coronary CT angiography: first experience with prospective ECG-gating. *Eur Heart J.* 2008; 29: 191-197.
 67. Steigner ML, Otero HJ, Cai T, et al. Narrowing the phase window width in prospectively ECG-gated single heart beat 320-detector row coronary CT angiography. *Int J Cardiovasc Imaging.* 2009; 25: 85-90.
 68. Fayad ZA, Nahar T, Fallon JT, et al. In vivo magnetic resonance evaluation of atherosclerotic plaques in the human thoracic aorta: a comparison with transesophageal echocardiography. *Circulation.* 2000; 101: 2503-2509.
 69. Hatsukami TS, Ross R, Polissar NL, Yuan C. Visualization of fibrous cap thickness and rupture in human atherosclerotic carotid plaque in vivo with high-resolution magnetic resonance imaging. *Circulation.* 2000; 102: 959-964.
 70. Skinner MP, Yuan C, Mitsumori L, et al. Serial magnetic resonance imaging of experimental atherosclerosis detects lesion fine structure, progression and complications in vivo. *Nat Med.* 1995; 1: 69-73.
 71. Toussaint JF, LaMuraglia GM, Southern JF, Fuster V, Kantor HL. Magnetic resonance images lipid, fibrous, calcified, hemorrhagic, and thrombotic components of human atherosclerosis in vivo. *Circulation.* 1996; 94: 932-938.
 72. Maynor CH, Charles HC, Herfkens RJ, Suddarth SA, Johnson GA. Chemical shift imaging of atherosclerosis at 7.0 Tesla. *Invest Radiol.* 1989; 24: 52-60.
 73. Soila K, Nummi P, Ekfors T, Viamonte M, Jr, Korman M. Proton relaxation times in arterial wall and atheromatous lesions in man. *Invest Radiol.* 1986; 21: 411-415.
 74. Stuber M, Weiss RG. Coronary magnetic resonance angiography. *J Magn Reson Imaging.* 2007; 26: 219-234.
 75. Fayad ZA, Fuster V, Fallon JT, et al. Noninvasive in vivo human coronary artery lumen and wall imaging using black-blood magnetic resonance imaging. *Circulation.* 2000; 102: 506-510.
 76. Kim WY, Stuber M, Bornert P, Kissinger KV, Manning WJ, Botnar RM. Three-dimensional black-blood cardiac magnetic resonance coronary vessel wall imaging detects positive arterial remodeling in patients with nonsignificant coronary artery disease. *Circulation.* 2002; 106: 296-299.
 77. Botnar RM, Stuber M, Lamerichs R, et al. Initial experiences with in vivo right coronary artery human MR vessel wall imaging at 3 tesla. *J Cardiovasc Magn Reson.* 2003; 5: 589-594.
 78. Kooi ME, Cappendijk VC, Cleutjens KB, et al. Accumulation of ultrasmall superparamagnetic particles of iron oxide in human atherosclerotic plaques can be detected by in vivo magnetic resonance imaging. *Circulation.* 2003; 107: 2453-2458.
 79. Wasserman BA, Smith WI, Trout HH, et al. Carotid artery atherosclerosis: in vivo morphologic characterization with gadolinium-enhanced double-oblique MR imaging initial results. *Radiology.* 2002; 223: 566-573.
 80. Yuan C, Kerwin WS, Ferguson MS, et al. Contrast-enhanced

- high resolution MRI for atherosclerotic carotid artery tissue characterization. *J Magn Reson Imaging*. 2002; 15: 62-67.
81. Tang TY, Muller KH, Graves MJ, et al. Iron oxide particles for atheroma imaging. *Arterioscler Thromb Vasc Biol*. 2009; 29: 1001-1008.
 82. Spuentrup E, Buecker A, Katoh M, et al. Molecular magnetic resonance imaging of coronary thrombosis and pulmonary emboli with a novel fibrin-targeted contrast agent. *Circulation*. 2005; 111: 1377-1382.
 83. Corti R, Fayad ZA, Fuster V, et al. Effects of lipid-lowering by simvastatin on human atherosclerotic lesions: a longitudinal study by high-resolution, noninvasive magnetic resonance imaging. *Circulation*. 2001; 104: 249-252.
 84. Deguchi JO, Aikawa M, Tung CH, et al. Inflammation in atherosclerosis: visualizing matrix metalloproteinase action in macrophages in vivo. *Circulation*. 2006; 114: 55-62.
 85. Gough PJ, Gomez IG, Wille PT, Raines EW. Macrophage expression of active MMP-9 induces acute plaque disruption in apoE-deficient mice. *J Clin Invest*. 2006; 116: 59-69.
 86. Schafers M, Riemann B, Kopka K, et al. Scintigraphic imaging of matrix metalloproteinase activity in the arterial wall in vivo. *Circulation*. 2004; 109: 2554-2559.
 87. Kolodgie FD, Petrov A, Virmani R, et al. Targeting of apoptotic macrophages and experimental atheroma with radiolabeled annexin V: a technique with potential for noninvasive imaging of vulnerable plaque. *Circulation*. 2003; 108: 3134-3139.
 88. Kietzelaer BL, Reutelingsperger CP, Heidendal GA, et al. Noninvasive detection of plaque instability with use of radiolabeled annexin A5 in patients with carotid-artery atherosclerosis. *N Engl J Med*. 2004; 350: 1472-1473.
 89. Rudd JH, Warburton EA, Fryer TD, et al. Imaging atherosclerotic plaque inflammation with [18F]-fluorodeoxyglucose positron emission tomography. *Circulation*. 2002; 105: 2708-2711.
 90. Worthley SG, Zhang ZY, Machac J, et al. In vivo non-invasive serial monitoring of FDG-PET progression and regression in a rabbit model of atherosclerosis. *Int J Cardiovasc Imaging*. 2009; 25: 251-257.
 91. Tahara N, Kai H, Ishibashi M, et al. Simvastatin attenuates plaque inflammation: evaluation by fluorodeoxyglucose positron emission tomography. *J Am Coll Cardiol*. 2006; 48: 1825-1831.
 92. Alexanderson E, Slomka P, Cheng V, et al. Fusion of positron emission tomography and coronary computed tomographic angiography identifies fluorine 18 fluorodeoxyglucose uptake in the left main coronary artery soft plaque. *J Nucl Cardiol*. 2008; 15: 841-843.
 93. Wykrzykowska J, Lehman S, Williams G, et al. Imaging of inflamed and vulnerable plaque in coronary arteries with 18F-FDG PET/CT in patients with suppression of myocardial uptake using a low-carbohydrate, high-fat preparation. *J Nucl Med*. 2009; 50: 563-568.
 94. Yuan C, Mitsumori LM, Beach KW, Maravilla KR. Carotid atherosclerotic plaque: noninvasive MR characterization and identification of vulnerable lesions. *Radiology*. 2001; 221: 285-299.
 95. Narula J, Garg P, Achenbach S, Motoyama S, Virmani R, Strauss HW. Arithmetic of vulnerable plaques for noninvasive imaging. *Nat Clin Pract Cardiovasc Med*. 2008; 5 Suppl 2: S2-10.
 96. Little WC, Constantinescu M, Applegate R, et al. Can coronary angiography predict the site of a subsequent myocardial infarction in patients with mild-to-moderate coronary artery disease? *Circulation*. 1988; 78: 1157-1166.
 97. Nobuyoshi M, Tanaka M, Nosaka H, et al. Progression of coronary atherosclerosis: is coronary spasm related to progression? *J Am Coll Cardiol*. 1991; 18: 904-910.
 98. Giroud D, Li JM, Urban P, Meier B, Rutishauer W. Relation of the site of acute myocardial infarction to the most severe coronary arterial stenosis at prior angiography. *Am J Cardiol*. 1992; 69: 729-732.
 99. Garcia JA, Movassaghi B, Casserly IP, et al. Determination of optimal viewing regions for X-ray coronary angiography based on a quantitative analysis of 3D reconstructed models. *Int J Cardiovasc Imaging*. 2008; 25: 455-462.
 100. Corti R. Noninvasive imaging of atherosclerotic vessels by MRI for clinical assessment of the effectiveness of therapy. *Pharmacol Ther*. 2006; 110: 57-70.